25th ABCM International Congress of Mechanical Engineering
October 20-25, 2019, Uberlândia, MG, Brazil

COB-2019-0527
LINEAR ELASTIC FRACTURE MECHANICS ANALYSIS OF A SQUARE HOLLOW STRUCTURAL STEEL SECTION PROFILE

Albert Santos
Thiago Doca
University of Brasília - Campus Universitário Darcy Ribeiro, Asa Norte, Brasília
santosalbt@gmail.com, doca@unb.br

Abstract. *A square hollow structural steel (HSS) section profile is usually used as structural element in mechanical structure. The square HSS can be used in the lifting mechanism of an agricultural implement, such as a flail mower, because it has high strength-to-weight ratio and uniform strength. The present work presents an analytical and numerical study of a square HSS with nominal size of 70x70x200 mm and wall thickness of 6,35 mm (made of carbon steel AISI 1020). The objective of this work is to perform a yield stress analysis and a fracture analysis using the finite element method. Organized as follows: the analytical formulation for validation of the numerical modeling, modeling steps, stress field analysis and crack analysis. In the yield stress analysis, a longitudinal stress is applied to determine the maximum force that can be applied, so that there is no yielding of the material. The fracture analysis aims to determine the largest length of a crack subjected to a load slightly lower than the maximum permissible load defined in the yield stress analysis. From the results were drawn curves that relate the correction factor and the crack length in order to obtain the stress intensity factor for different loads. .*

Keywords: *Finite Element Method, Crack, Stress Intensity Factor.*

1. INTRODUCTION

In the design of an agricultural implement it is necessary to consider the presence of cracks in the mechanical structure as a consequence of the great loads generated by the weight of the implement.

A flail mower is an agricultural implement that usually needs to be lift by an arm or by a linkage mechanism, as shown in Fig. 1a. These mechanisms can be made of square steel tubes. A square hollow structural steel (HSS) section is commonly used when a balance is required between strength and functionality in structural and mechanical applications. This tube is widely used because it can be straight-cut when joining to other flat surfaces, and minimal edge preparation is required for joining and welding. Austube Mills (2018)

(a) Commercial flail mower.

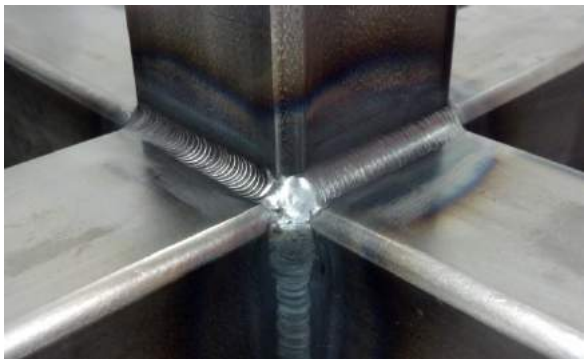

(b) Welding of four square tube arms with a single tube.

Figure 1: Example of a tube used in the linkage mechanism.

In the welding process there are several factors that can contribute to the appearance of these cracks. The causes of these cracks may be related to the following factors: chemical composition of the welding wire; small weld bead; base material not previously examined ; welding over slag; narrow weld joint; welding current too low; residual stresses; temperature changes during the welding process; deformation from the cooling process; etc. Thus, the objective of this work is to study the behavior of a square steel tube in the presence of a central through crack in one of its surfaces.

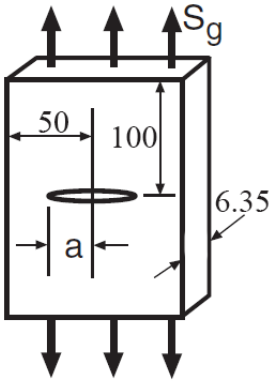

Figure 2: Central crack in a finite plate under uniaxial stress (units in mm). Figure adapted from figure 8.12 in Dowling (2012)

The fracture mechanics is responsible for studying the relationships between the properties of the materials, the presence of cracking discontinuities, the stress level and crack propagation mechanisms. The linear elastic fracture mechanics, LEFM, assume, initially, that the material is elastic, isotropic and linear. In this way the tensile field near the crack tip is calculated using the theory of elasticity.

The loading can act in a crack of three fundamental modes, affecting in different ways the cracked surface. The fundamental modes are: mode I (opening mode, traction of crack surfaces), mode II (sliding mode, plane loading) and mode III (tearing mode, anti-plane loading). In the present work the mode I of relative movement of the surface of the crack was treated (tensile stress normal to the plane of the crack). Santos (2018)

A measure of the severity of a crack situation as affected by crack size, stress, and geometry is called stress intensity factor, K. The stress intensity factor characterizes the stress field in the crack tip region, and helps to predict the fracture condition and remaining life. It is important to know the maximum allowable stress to determine when a crack starts to grow. The fracture toughness (K_{IC}, critical stress intensity factor) indicates the maximum value of K so that there is no collapse of the mechanical component. According to this, crack stability can be determined by comparing K and K_{IC}. Ali *et al.* (2014) Dowling (2012)

Initially it is aimed to determine the uniaxial force that the tube supports so that it does not present plastic behavior. For this, the von Mises stress must be lower than the yield strength. After determining this force we can apply it in a cracked tube and find the maximum crack length so that the tube does not fail.

2. MATERIAL AND METHODS

2.1 Analytical Approach

In order to validate the model, a case with analytical solution for loading in Mode I is presented: central crack in a finite plate under uniaxial stress.Thus, it is possible to compare the results obtained through analytical and numerical solutions. In this way it is possible to define some criteria: element size, element shape, boundary conditions and the interaction specifications between the crack and the body.

The stress intensity factor for a central crack in a finite plate under uniaxial stress is given by equation 1. Tada *et al.* (1973)

$$K = F(\frac{a}{b})S_g\sqrt{\pi a} \tag{1}$$

The therms $F(\frac{a}{b})$ and S_g are determined according to equations 2 and 3, respectively.

$$F(\frac{a}{b}) = \frac{1 - 0.5(\frac{a}{b}) + 0.326(\frac{a}{b})^2}{\sqrt{1 - (\frac{a}{b})}} \tag{2}$$

$$S_g = \frac{P}{2bt} \tag{3}$$

The width $2b$ is 100 mm, the thickness t is 6.35 mm and the force P is 7 kN. The semi-length $2a$ of the crack varies between 10 and 90 mm. Figure 2 shows the evaluated model.

Table 1: Mechanical properties of AISI 1020 Carbon Steel. Doca and Pires (2014)

	AISI 1020 Carbon Steel
Specific Mass, ρ	7870 kg/m^3
Young's Modulus, E	203 *GPa*
Poisson's Ratio, ν	0,3
Yield Strength, σ_y	350 *MPa*
***Fracture Toughness,** K_{IC}	51 $MPa\sqrt{m}$

2.2 Numerical Approach

For the numerical approach the finite element commercial program Abaqus 6.14 was used. The computer used in the simulations has an Intel(R) Core(TM) i7-5500U @ 2.4GHz,with 8.00 GB RAM and 64-bit operating system, x64 based processor.

For better organization this section is divided into four subsections: Mesh Convergence Study; Geometry, Material and Section; Assembly and Interaction; Load, Boundary Conditions and Mesh.

Mesh Convergence Study: It is necessary to perform a convergence study using the results obtained from de analytical solution presented in the previous section (central crack in a semi-finite plate under uniaxial tension) to define the simulation parameters. The plate's dimensions are shown in Fig. 2.

An iterative process was performed in order to optimally determine the main simulation parameters. The parameters show below were determined after a series of simulations that aimed to find the numerical values that were closest to the analytical result.

The properties of the material used in the simulations of this work are presented in Tab. 1. The value of K_{IC} was not found in the literature, thus a K_{IC} of a similar material, AISI 1045 carbon steel was adopted.NTIS (1973)

To evaluate the Mode I stress intensity factor of the crack the method of the contour integral was used. In the interaction module the seam was assigned to the partition created in the center of the body. The first step in setting a crack is to determine the front of the crack. The crack front is the forward part of the crack, edge at the end of the partition. The elements inside the crack front and one layer of elements outside the crack front are used to compute the first contour integral.

A strain singularity for an elastic fracture was included in the contour integral calculation. For this purpose the value of the parameter *midside node parameter* must be changed to 0.25. The box *Collapsed element side, single node* should also be checked. SIMULIA ABAQUS 6.14 (2015)

In the *step module* the *history output request* was modified to add more layers to compute the contour integral. The number of contours was defined as 10 and the stress intensify factor was request(the maximum energy release rate was adopted as a criterion for crack initiation).

In the *load module* a force of 7 kN was applied on the top surface of the plate and a symmetry relation on the y-axis was applied on the bottom surface of the plate as shown in Fig 3a.

Finally we must specify the element shape and the element size that will be applied in the mesh.The ideal configuration found is shown in Fig. 3b. In the *seed part instance* editor the approximate global size was defined as 2 mm. Subsequently in the editor *assign mesh controls* hexagonal-sweep-media axis elements were applied to the body. In the contour region wedge-sweep elements were applied and it was also determined that the radius of this region is 2 mm.

The results of Tab. 2 show that the numerical results are close to the analytical results, with a maximum error of 3,14%. When considering the computational cost we can consider these negligible errors.

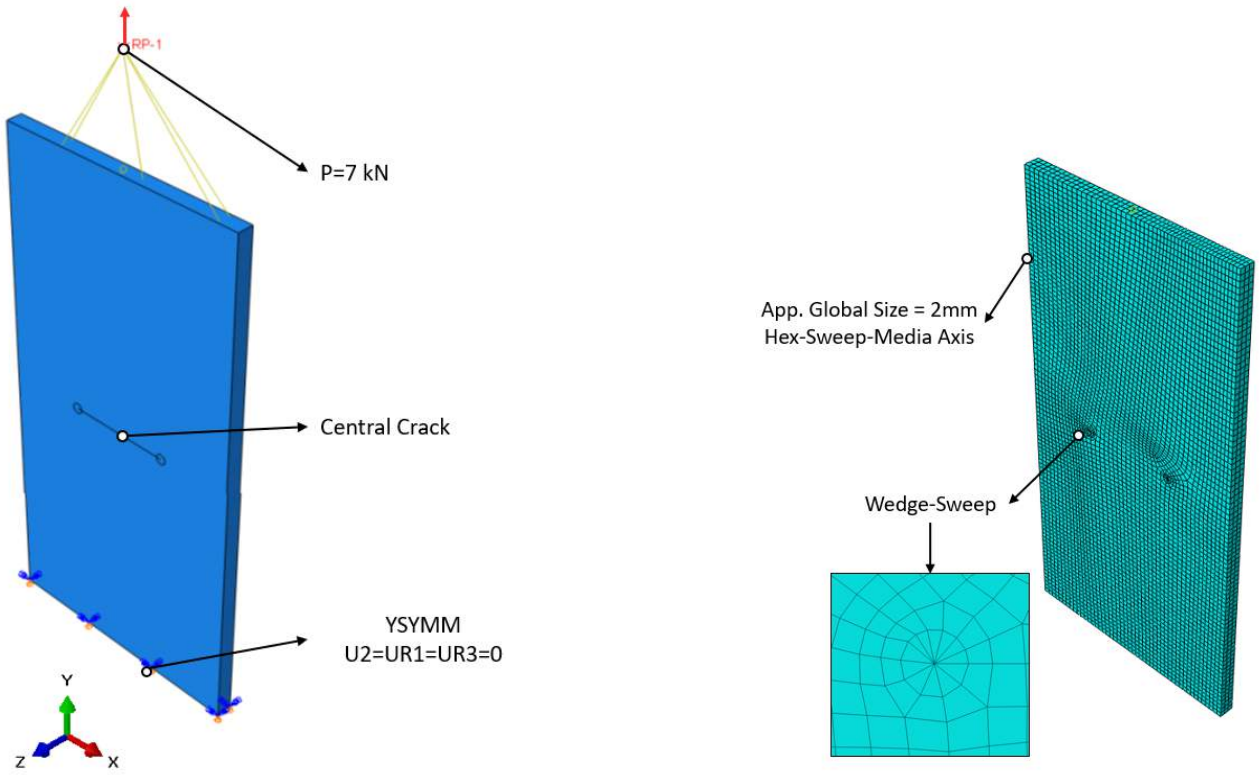

(a) Load and boundary conditions. (b) Mesh and zoom at the crack tip.

Figure 3: Load, boundary conditions and mesh applied (2a = 40 mm).

Table 2: Stress intensity factors results and comparison between analytical and numerical solution.

2a $[mm]$	K $[MPa\sqrt{m}]$		**Error** $[\%]$
	Numerical	**Analytical**	
10	1,363	1,388	1,85
15	1,765	1,711	3,14
20	2,002	1,995	0,37
25	2,295	2,259	1,60
30	2,579	2,515	2,52
35	2,838	2,773	2,35
40	3,111	3,040	2,35
45	3,395	3,324	2,15
50	3,702	3,633	1,92
55	4,065	3,978	2,18
60	4,464	4,374	2,08
65	4,935	4,839	1,98
70	5,450	5,404	0,84
75	6,144	6,117	0,44
80	7,069	7,066	0,04
85	8,356	8,430	0,88
90	10,441	10,670	2,15

The graph shown in Fig. 4 shows the alignment of the analytical and numerical curves.

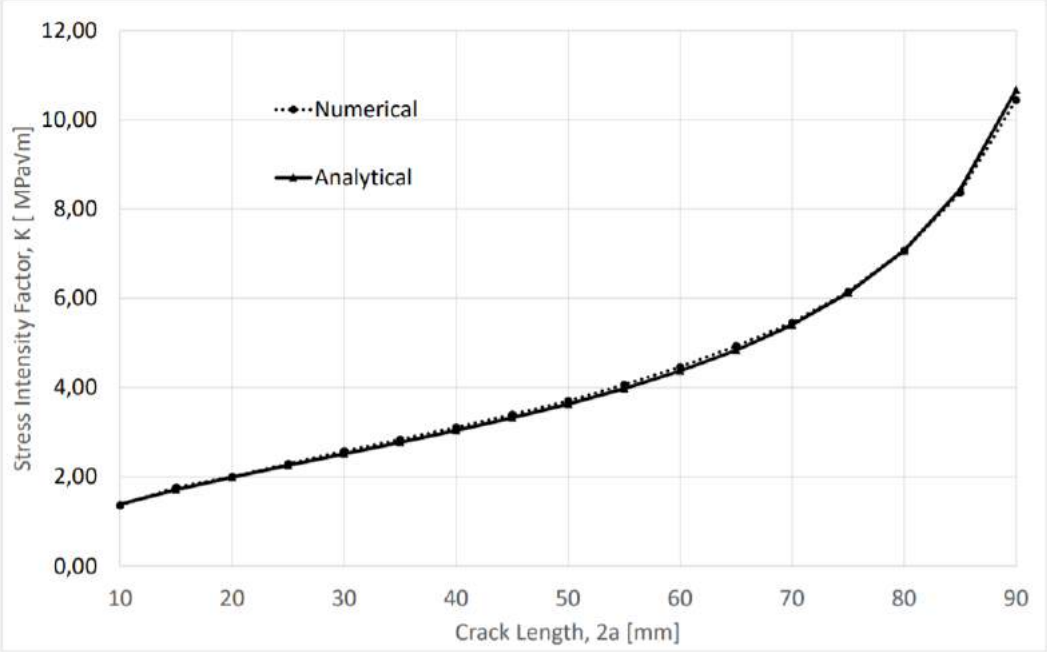

Figure 4: Analytical and numerical approach for a cracked plate under tension.

Geometry, Material and Section: The square steel tube dimension is shown in Fig. 5a. Figure 5b shows the partitions created to allow creation of the mesh and insertion of the crack. A homogeneous and solid section with AISI 1020 carbon steel (Tab. 1) was assigned to the whole body.

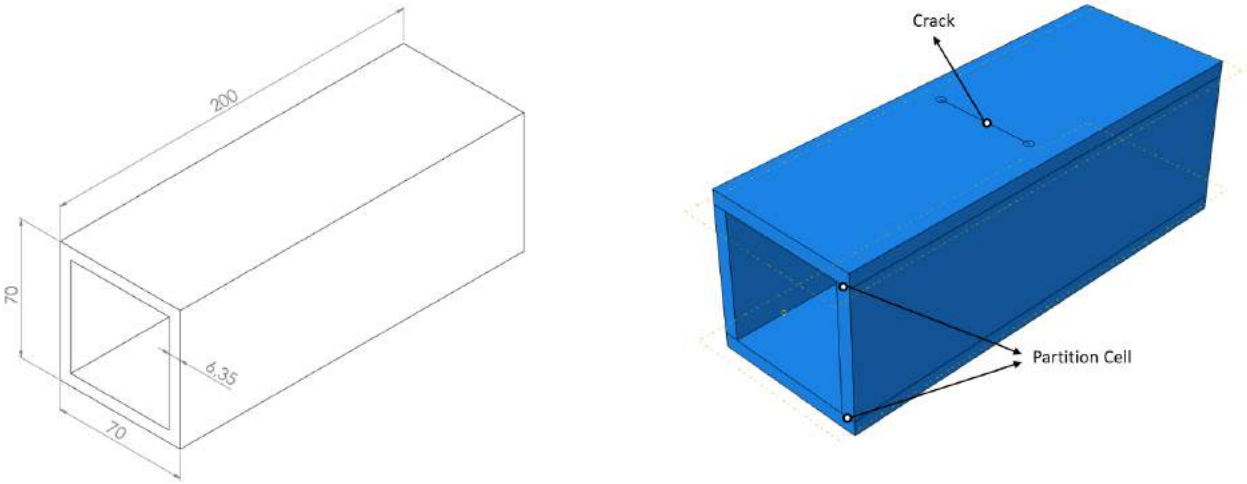

(a) Body dimensions (units in mm). (b) Body partitions.

Figure 5: Geometry and partitions of the square steel tube. (2a = 50 mm).

Assembly and Interaction: First a seam is assigned to the partition created in the center of the structural steel. Then two crack fronts are selected and the crack extension direction is defined by the q vectors, as shown in figure 6.

A strain singularity must be added, as explained in the previous section. For this purpose the value of the parameter *midside node parameter* must be changed to 0.25 and the box *Collapsed element side, single node* should be checked.

The *history output request* editor is modified to add more layers to compute the contour integral. The number of contours was defined as 10 and the stress intensify factor was request(the maximum energy release rate was adopted as a criterion for crack initiation), as shown in the convergence study.

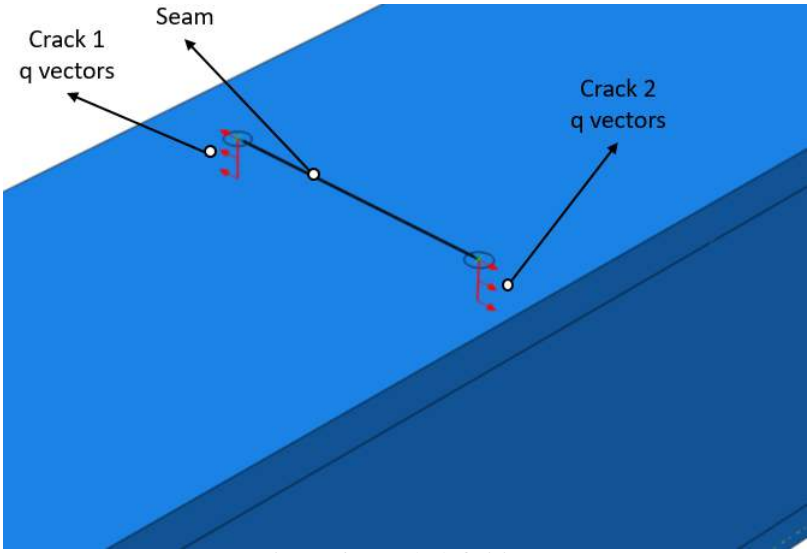

Figure 6: Crack definitions.

Load, Boundary Conditions and Mesh: Initially, it is desired to know the applied force that initiates a plastic behavior. A simple simulation is performed and it was found that the maximum force supported before the material has plastic deformations is 350 kN. Thus, in the *load module* a force of 350 kN was applied at one end of the body and a encastre was applied at the other end as shown in Fig. 7a.

On the top surface was applied hexagonal-sweep-advancing axis elements to avoid mesh distortion in the vicinity of the contour region. In the contour region wedge-sweep elements were applied and it was also determined that the radius of this region is 2 mm. In the other areas hexagonal-structural elements were applied. Figure 7b shows the regions where each element type was applied.

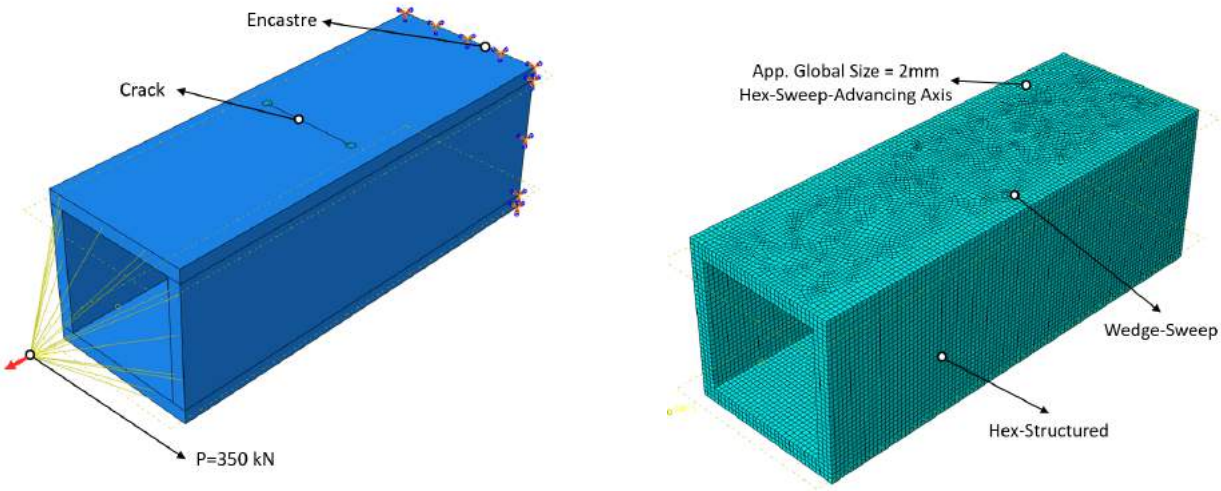

(a) Load and boundary conditions. (b) Mesh inputs.

Figure 7: Load, boundary conditions and mesh applied (2a = 50 mm)..

After the simulation in the finite element program, we obtain the results presented in chapter 3.

3. RESULTS AND DISCUSSION

Figure 8 shows the von Mises stress distribution at the crack tips as well as crack opening. We can see that the von Mises stress value tends to infinity for an infinitesimal element (expected singularity).

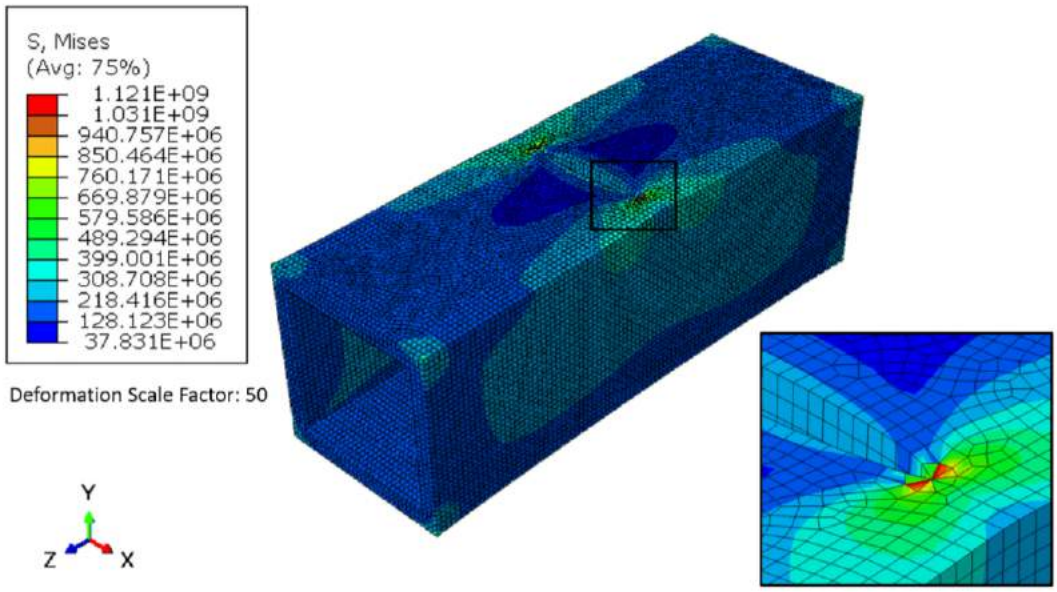

Figure 8: von Mises stress field distribution near the crack tip.

Table 3 shows the stress intensity factor for a tube subjected to a stress slightly below the material yield strength. This stress is generated by the 350 kN uniaxial force applied in the axial direction of the body. This allows us to determine the maximum crack size for this loading so that no fracture occurs.

Table 3: Correction factor and stress intensity factor for a cracked square steel tube under tension.

2a $[mm]$	10	15	20	25	30	35	40	45	50
K $[MPa\sqrt{m}]$	27,432	34,079	39,944	45,169	50,458	55,539	60,927	66,435	71,731
Correction Factor	1,011	1,026	1,041	1,053	1,074	1,094	1,123	1,154	1,182

Figure 9 shows the curve found when plotting the data presented in Tab. 3. Analyzing the graph we can see that the maximum length allowed by the AISI 1020 steel is 30 mm.

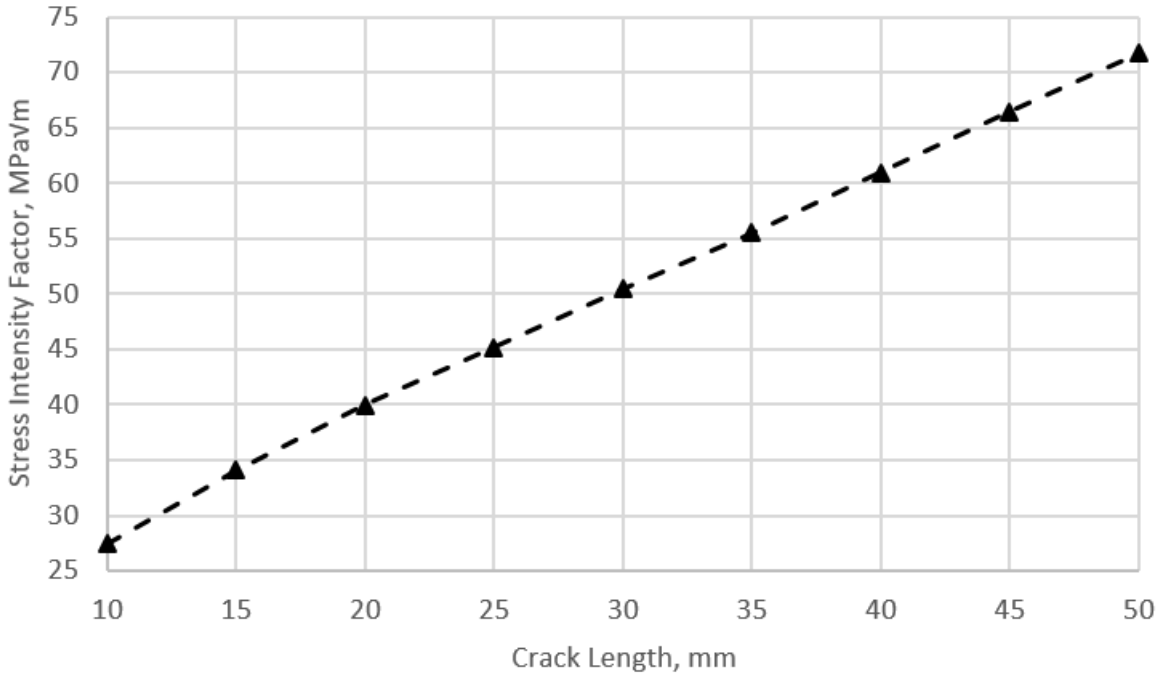

Figure 9: Stress intensity factor for a cracked square steel tube under tension.

To eliminate load dependence, the correction factor for Mode I stress intensity factor is isolated from equation 1, as

shown in the equation 4.

$$F = \frac{K}{S_g\sqrt{\pi a}} \tag{4}$$

Assigning different values of a and K in equation 4, we obtain a set of data that define the correction factor.Figure 10 shows the relation between the correction factor and the crack length for a cracked square steel tube under tension.

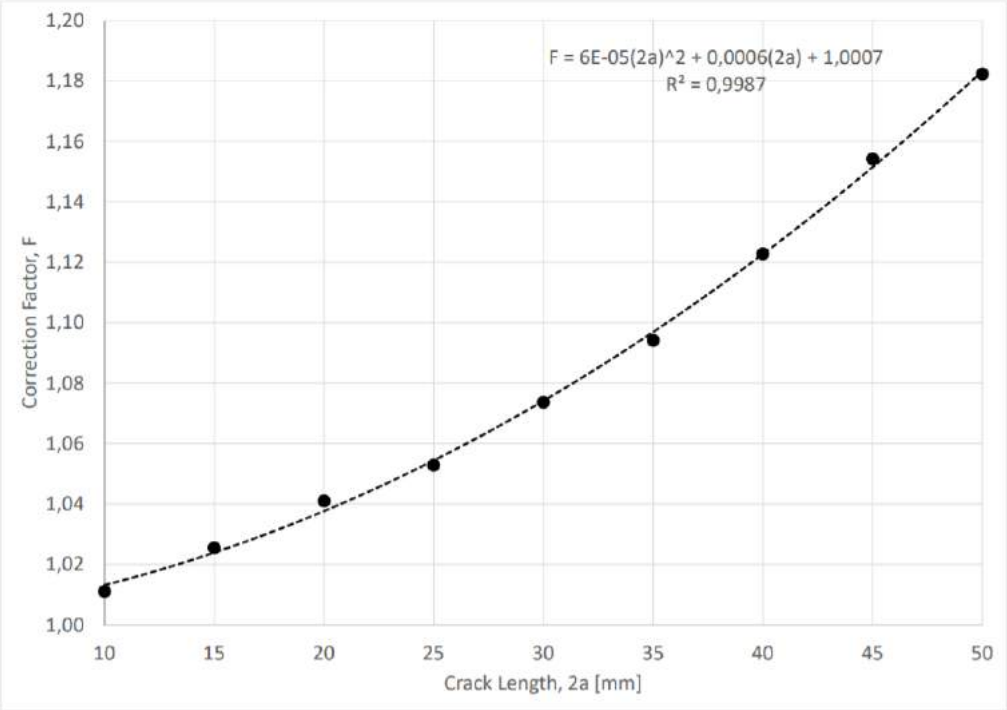

Figure 10: Correction factor for a cracked square steel tube under tension.

4. CONCLUSION

It can be verified that the numerical solutions found by the finite element program, in the cases discussed here, are in accordance with the results obtained by the analytical model.

The numerical results presented small relative errors (maximum error of 3%) for the convergence study shown. When evaluating the computational cost, represented by the numerical simulation time elapsed, it is seen that the parameters adopted are sufficient for the cases presented in this work.

In the fracture analysis the linear elastic fracture mechanics is used for the calculation and evaluation of the analytical and numerical results. The maximum permissible length of the crack is defined by graph (Fig. 9) which relates the stress intensity factor and the crack length. We can then define that the maximum permissible crack length is 30 mm for a square steel tube when subjected to a 100 kN force and for a material with a fracture toughness of 51 MPa$\sqrt{m}$.

In order to eliminate the dependence of the load, a graph was also plotted that relates the correction factor and crack length.

5. REFERENCES

Ali, Z., Meysam, K., AsadiIman, B.A. and Yashar, B., 2014. "Finite element method analysis of stress intensity factor in different edge crack positions and predicting their correlation using neural network method". *Research Journal of Recent Sciences*, Vol. 3, No. 2, pp. 69–73.

Austube Mills, 2018. "Square Hollow Sections". URL `http://www.austubemills.com.au`. Online.

Doca, T. and Pires, F.A., 2014. "Analysis of a cylinder-to-flat contact problem at finite elasto-plastic strains". *Tribology International*, Vol. 79, pp. 92–98.

Dowling, N.E., 2012. *Mechanical behavior of materials: engineering methods for deformation, fracture, and fatigue*. Pearson.

NTIS, 1973. "Plane strain fracture toughness (kic) data handbook for metals".

Santos, A., 2018. "Estudo analítico e numérico de mecanismos de união de tubulações". *Universidade de Brasília*.

SIMULIA ABAQUS 6.14, 2015. "Getting Started with Abaqus: Interactive Edition". URL `http://abaqus.software.polimi.it/v6.14/books/gsa/default.htm?startat=ch11.html`. Online.

Tada, H., ASME and Irwin, G.R., 1973. *Stress Analysis of Cracks Handbook, Third Edition*.

6. RESPONSIBILITY NOTICE

Albert Santos is the only responsible for the printed material included in this paper.